



Research article

Metastases or benign adrenal lesions in patients with histopathological verification of lung cancer: Can CT texture analysis distinguish?

Michael Brun Andersen^{a,b,c,*}, Uffe Bodtger^{d,e}, Iben Rahbek Andersen^b, Kennet Sønderstgaard Thorup^b, Balaji Ganeshan^f, Finn Rasmussen^b

^a Department of Radiology Zealand University Hospital, Roskilde, Denmark

^b Department of Radiology Aarhus University Hospital, Skejby, Denmark

^c Copenhagen University Hospital, Gentofte, Denmark

^d Pulmonary Research Unit (PLUZ), Department of Internal Medicine, Zealand University Hospital, Naestved, Denmark

^e Institute for Regional Health Research, University of Southern Denmark, Odense, Denmark

^f Institute of Nuclear Medicine, University College London, United Kingdom



ARTICLE INFO

Keywords:

Computed tomography
Texture analysis
Lung cancer
Adrenal gland

ABSTRACT

Introduction: Distant metastases are found in the many of patients with lung cancer at time of diagnosis. Several diagnostic tools are available to distinguish between metastatic spread and benign lesions in the adrenal gland. However, all require additional diagnostic steps after the initial CT. The purpose of this study was to evaluate if texture analysis of CT-abnormal adrenal glands on the initial CT correctly differentiates between malignant and benign lesions in patients with confirmed lung cancer.

Materials and methods: In this retrospective study 160 patients with endoscopic ultrasound-guided biopsy from the left adrenal gland and a contrast-enhanced CT in portal venous phase were assessed with texture analysis. A region of interest encircling the entire adrenal gland was used and from this dataset the slice with the largest cross section of the lesion was analyzed individually.

Results: Several texture parameters showed statistically significantly difference between metastatic and benign lesions but with considerable between-groups overlaps in confidence intervals. Sensitivity and specificity were assessed using ROC-curves, and in univariate binary logistic regression the area under the curve ranged from 36 % (Kurtosis 0.5) to 69 % (Entropy 2.5) compared to 73 % in the best fitting model using multivariate binary logistic regression.

Conclusion: In lung cancer patients with abnormal adrenal gland at imaging, adrenal gland texture analyses appear not to have any role in discriminating benign from malignant lesions.

1. Introduction

Globally, lung cancer is the most common cause of cancer death [1]. Distant metastases at time of diagnosis is found in almost half of all patients with non-small cell lung cancer (NSCLC) and a higher proportion in small cell lung cancer (SCLC) [2]. A frequent site of metastatic spread is the adrenal glands. The prevalence of benign adrenal lesions is 3–10 % in the background population [3]. 4–7 % of potentially resectable patients have adrenal masses of which only a minority is due to

metastatic spread [4,5].

Several imaging methods are available for assessment of malignancy in adrenal masses observed at the initial, contrast-enhanced, diagnostic CT chest and abdomen, but all require additional CT, MRI, or PET/CT imaging procedures. *CT washout measurement* uses a non-contrast CT, a contrast-enhanced CT after 1 min and a late contrast-enhanced CT after 15 min to calculate either an absolute washout >60 %, or a relative washout >40 % [6]. *In-phase/out-phase MRI* can depict microscopic lipid as a drop in signal on out-phase scans [7]. Using *PET/CT*, non-functional

Abbreviations: NSCLC, non-small cell lung cancer; SCLC, small cell lung cancer; 18-FDG, 18-FluoroDeoxyGlucose; EUS, endoscopic ultrasound; EUS-B, endobronchial ultrasound; CTTA, computed tomography texture analysis; ML, machine learning; AI, artificial intelligence; ROI, region of interest; ICC, intraclass correlation.

* Corresponding author at: Copenhagen University Hospital, Radiology Department, Gentofte Hospitalsvej 1, 2900 Hellerup, Denmark.

E-mail addresses: Michael.brun.andersen@regionh.dk (M.B. Andersen), ubt@regionsjaelland.dk (U. Bodtger), iben.rahbek.andersen@rm.dk (I.R. Andersen), kennthor@rm.dk (K.S. Thorup), B.ganeshan@ucl.ac.uk (B. Ganeshan), Finnrasm@rm.dk (F. Rasmussen).

<https://doi.org/10.1016/j.ejrad.2021.109664>

Received 22 February 2021; Received in revised form 10 March 2021; Accepted 15 March 2021

Available online 18 March 2021

0720-048X/© 2021 The Authors. Published by Elsevier B.V. This is an open access article under the CC BY license (<http://creativecommons.org/licenses/by/4.0/>).

adrenal adenomas show no or low uptake of 18-FluoroDeoxyGlucose (18-FDG), whereas functional adenomas and malignant lesions have high 18-FDG uptake [8].

Correct staging of lung cancer is pivotal for optimal treatment. An enlarged adrenal gland may be the only sign of cancer dissemination in otherwise local or locally advanced and thus possibly curable disease. The left adrenal gland is readily available for tissue sampling using endoscopic ultrasound (EUS) using either the conventional EUS endoscope or the smaller endoscope designed for endobronchial ultrasound with a high diagnostic yield and few adverse events (EUS-B) [9]. The right adrenal gland is often difficult to biopsy by endoscopy. Transcutaneous biopsy - guided by CT or ultrasound - is possible from both adrenal glands, but with a risk of traversing the lung bases, spleen or liver. This is avoidable by employing hydro-dissection and using the paravertebral space [10]. These invasive examinations are resource consuming, and transcutaneous sampling is associated with adverse events. Thus, there is a need for the development of simple rule-in or rule-out test to direct resource allocation in these patients who awaits treatment for a potentially fatal disease.

CT Texture analysis (CTTA) is a technique that provides quantitative information about image pixel intensity and distribution (subtle heterogeneity not perceptible to the naked eye). In recent years, CTTA has been increasingly applied in radiology research as part of radiomics and machine-learning (ML) /Artificial-intelligence (AI) techniques within computer-aided diagnosis [11]. By definition of texture parameters, CTTA may offer information about the tissue characteristics (heterogeneity), and its utility has been proven especially in the diagnosis/disease-severity, treatment-response/prediction and prognosis of a number of tumors [12,13].

Concerning adrenal lesions, CTTA has shown some promise in differentiating malignant from benign lesions. However, external validity of the findings in relation to lung cancer is hampered by small samples, single-center design, or non-lung cancer population [14–17].

The purpose of this study is to evaluate if texture analysis can differentiate between malignant and benign adrenal masses in patients with diagnosed lung cancer.

2. Materials and methods

2.1. Design, patients, and definition of a true negative adrenal biopsy

This study was a retrospective study, following the STROBE guidelines, of all patients who had undergone EUS or EUS-B procedure between December 2009 and February 2016 at the Diagnostic Unit, Department of Internal and Respiratory Medicine, Zealand University Hospitals of Naestved or Roskilde, two tertiary departments performing workup of suspected lung cancer. In these units, EUS or EUS-B is the modality of choice to investigate possible left adrenal malignancy. CT- or ultrasound-guided sampling constitutes less than 2% of all adrenal gland biopsy procedures.

Patients were included in the present study if CT or PET-CT showed suspicion of lung cancer, enlarged adrenal gland(s) and EUS/EUS-B procedure was performed. Exclusion criteria where: no or inconclusive adrenal gland cytopathology, non-lung cancer pathology, absent CT, or CT artefacts obscuring the texture analysis of the adrenal glands (Fig. 1).

A true benign result of adrenal biopsy was defined as: no malignant cells in the biopsy specimen, and no progression of adrenal gland size at CT at least 6 months after the initial, suspicious CT.

2.2. Primary outcome

Statistically significant differences in CTTA parameters between malignant and benign adrenal glands were considered the primary outcome.

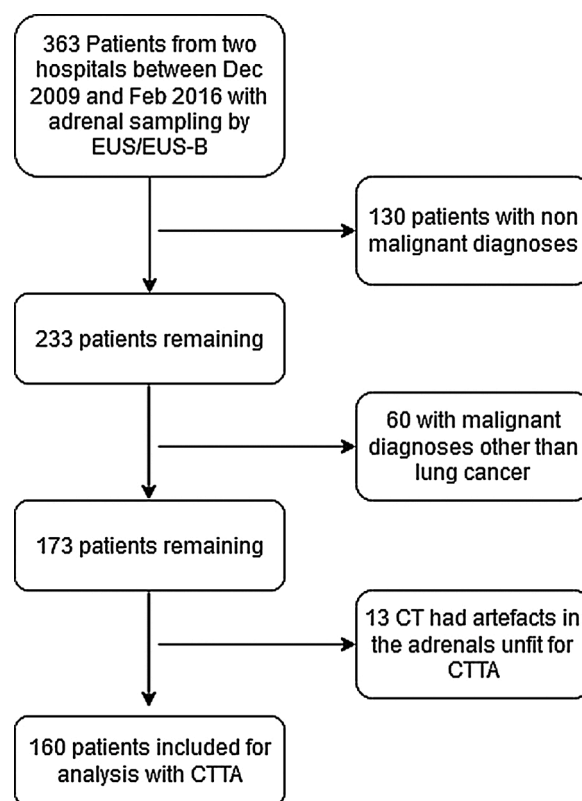


Fig. 1. A flowchart of inclusion, exclusion and the overall study design.

2.3. Contrast-enhanced CT imaging protocol

CT was performed with multiple-row detector CT scanners. Six different CT systems were used in this study (Table 1). However, a standard protocol was used with the following CT acquisition parameters: maximum collimation of 64 × 0.625 mm for Philips and Siemens scanners and 64 × 0.5 mm for the GE scanner, kV 120, dose modulation

Table 1

Patient demographics including age, sex, primary tumor pathology, adrenal gland pathology and type of scanner used for performing CT workup.

Table 1: Demographics		
Age	Years of age	68.6 (CI95 % 67.3–70.0)
Sex	Male	64
	Female	96
Primary tumor pathology	Adenocarcinoma	85
	Squamous Cell Carcinoma	42
	Neuroendocrine Tumor	10
	Unclassified NSCLC	7
	SCLC	16
Adrenal gland pathology	Benign	89
	Adenocarcinoma	38
	Squamous Cell Carcinoma	14
	Neuroendocrine Tumor	4
	Unclassified NSCLC	6
	SCLC	9
Scanner type	GE Medical Systems	11
	Philips Brilliance 16P	5
	Philips Brilliance 64	70
	Philips ICT 256	8
	Siemens Biograph 40	10
	Siemens Definition AS	1
	Siemens Somatom Edge	15

with mAs/slice 71–768 (scanner dependent), rotation time 0.75, reconstruction thickness 2–5 mm, increment 2–5 mm, pitch 1.078, FOV 20–50 cm and matrix 512×512 . CT examinations included the chest and the upper abdomen. Iomeprol 300 mg/mL (Iomeron® 300; Bracco Imaging, Milan, Italy), or iohexol 300 mg/mL (Omnipaque® 300; GE Healthcare), was injected intravenously in standard doses of 100 ml with an injection rate of 3 ml/sec. CT was performed after a delay of 70 s for the chest and upper abdomen (portalvenous phase) after initiation of contrast administration.

2.4. Adrenal sampling by EUS or EUS-B

The left adrenal gland was sampled in an ambulatory setting by an experienced operator using either the gastrointestinal (EUS; Olympus GF-UC160 P OL5) or the bronchial echoendoscope (EUS-B; Olympus BF-UC180 F; both: Olympus Medical Systems Europe Ltd, Hamburg, Germany) under conscious sedation using intravenous midazolam and fentanyl [18,19]. EUS-B is increasingly popular as adrenal gland sampling can be performed with the same scope and in the same session as mediastinal staging [9,18]. Two or more fine-needle aspiration biopsies were performed, assuring sufficient material for preparation of both smears and cell blocks [9].

2.5. CTTA of adrenal glands

CTTA was performed using TexRAD, a research software (TexRAD Ltd, Cambridge, UK) The technique comprised an image filtration-histogram approach; in which an initial filtration step using a Laplacian of Gaussian band-pass filter (non-orthogonal Wavelet) was employed/applied? to extract and enhance features of different size

based on the spatial scale filter values varying from 1.4 to 4.1 mm in diameter. Following image filtration, each filtered image texture map was quantified using histogram parameters such as Mean, Entropy and Uniformity (Fig. 2). These parameters are explained in detail by Miles et al. [11].

A radiologist in training with more than 5 years' experience in the use of the TexRAD software performed the analysis. The radiologists were blinded to all patient identifiers and clinical data as well as results from CT and tissue sampling. Region of Interests (ROI's) were delineated using Philips Intellispace Tumor Tracking, Best, Holland. A ROI including the total circumference of the adrenal gland was delineated and applied in the volume measurements. Furthermore, the single slice with the largest cross-section area was analyzed separately. The ROI's were saved as RT structure sets and transferred into the TexRAD software, where a semi-automated approach further refined the ROI enclosing the primary tumor to exclude surrounding fat using a threshold procedure removing pixels with an attenuation value below -50 HU. Another consultant radiologist with more than 7 years' experience in the use of the TexRAD software performed analysis on 35 random cases for inter-observer variability and reliability statistics.

2.6. Statistical analysis

Statistical analysis was performed in STATA 14 (Statacorp®, College Station, Texas, USA). A p-value <0.05 was considered statistically significant.

All texture parameters were checked for Gaussian distribution by Q-Q plots and the Shapiro-Wilks test. Normally distributed data were presented as mean (standard deviation) and inter-group differences analyzed with Student's T-test. In case of absent normal distribution,

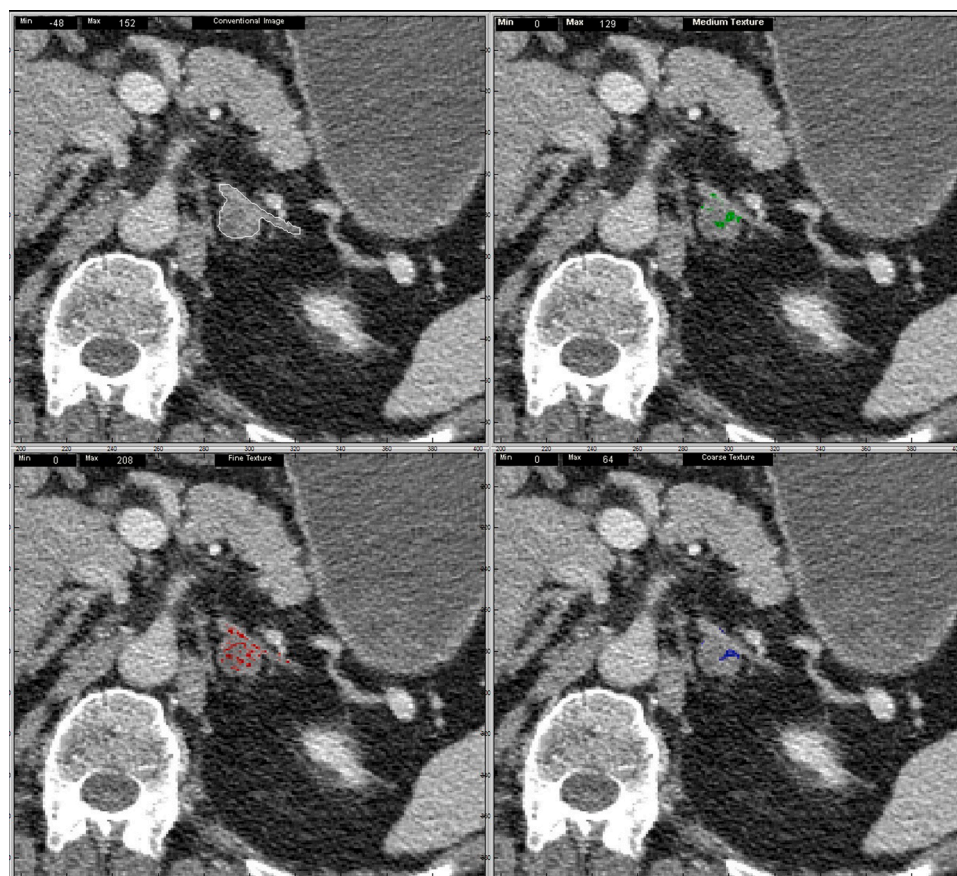


Fig. 2. TexRAD research software showing the drawn ROI (Top left) delineating the left adrenal and the representation of fine (Bottom left), medium (Top right) and coarse textures (Bottom right). TexRAD indicates grading of textures in color: Red = fine, green = medium and blue = coarse.

data were presented as median (range), and inter-group differenced analyzed with Mann-Whitney's *U* test

Inter-observer variability of the texture parameters where assessed by calculating the intra-class correlation coefficient (ICC) and values above 0.75 were considered good while values above 0.9 were considered excellent reliability. Only parameters with values above 0.75 were used in further analyses (Supplemental material 1 and 2).

In normally distributed data mean, standard error and 95 % confidence intervals were calculated in parameters with statistically significant difference between malignant and benign outcome. In case of non-normally distributed data median and range were calculated.

All parameters with statistically significant difference between the malignant and benign outcome, and with good or excellent stability was individually assessed with univariate binary logistic regression. Based on this test, all parameters were tested for correlation, and parameters showing no correlation but significantly discriminated outcomes in the univariate analysis were included in a multivariate analysis model. Furthermore, a nomogram based on the multivariate model was generated.

3. Results

3.1. Patients

Fig. 1 presents the preliminary flow of patients included. In the inclusion period, 363 patients underwent adrenal gland sampling during EUS or EUS-B: 233 were diagnosed with cancer, and 173 diagnosed with primary lung cancer. Yet, artefacts on CT made 13 patients unfit for CTTA, why a total of 160 patients (96 females and 64 males; mean age, 68.6 ± 8.7 years) where included. Table 1 lists basic demographics and final diagnosis.

3.2. Assessment of distribution

Only four texture analysis parameters were normally distributed (see Tables 2 and 3), whereas all remaining parameters were not normally distributed. This includes subgroup analysis based on malignant or benign adrenal pathology - thus only non-parametric statistics were

applied to these.

3.3. Results of adrenal biopsy sampling

Table 1 present 71 patients (44 %) diagnosed with metastatic spread to the left adrenal gland, mostly due to adenocarcinoma (53 %). 10 (6%) patients presented with benign adrenal biopsy and died or had no CT > 6 months after initial CT.

3.4. CT texture analysis of malignant and benign adrenal lesions

The volume measurements/assessments are presented in Table 2. We found statistically significant differences concerning Mean on unfiltered data, Kurtosis on low filtration levels (0.5 and 1.0) and - for higher filtration levels - also Uniformity and Entropy.

The single slice measurements/assessments are presented in Table 3. We found no statistically significant differences in kurtosis between the groups/outcomes, whereas Entropy and Uniformity showed statistically significant in most filtration levels. Unfiltered Mean and Mean of Positive Pixels also show statistically significant differences between the outcomes, the latter in several filtration levels. Both entropy and mean are found to be higher in the metastatic group compared to the benign (Fig. 3). Only uniformity shows a higher value in the benign group compared to the metastatic group.

3.5. Inter-observer variability of texture parameters

In the volume measurements, 8 of the 17 parameters showed excellent, 4 good, and 5 poor reliability (ICC single measures) thus 71 % showed good or excellent reliability. For single slice measurements, the comparable numbers were 6, 7, and 6 of the 19 parameters, thus 68 % showed good or excellent reliability.

When estimating/assessing the average measures for ICC we found a higher degree of correlation between readers in the single slice measures compared to volume measurements in which 82 % have good or excellent reliability for volume measures and 100 % for single slice measurements (supplemental material 1 and 2, also showing 95 % CI intervals).

Table 2

Mean texture parameters for the entire volume of the adrenal gland. Mean/Median, Std. error/range and 95 % CI interval split on benign and malignant groups.

Table 2 Mean texture parameters for volume										
Filter	Texture Parameter	Distribution	Mean/Median dependent on distribution							
			Benign				Malignant			
			Mean	Range	Std. Error	95 % CI	Mean	Range	Std. Error	95 % CI
Unfiltered	Mean	Gaussian	42.65811	-	1.407181	39.86894 to 45.42729	51.01786	-	1.875227	47.3143 to 54.72143
Unfiltered	Mean Positive Pixels	Gaussian	50.76672	-	1.17176	48.4525 to 53.08094	57.37339	-	1.541555	54.32882 to
0.5	Kurtosis	Skewed	0.27451	-0.4488842 to 5.119796	-	-	0.1880189	-0.294163 to 30.1452	-	-
1.0	Kurtosis	Skewed	0.4443989	-0.3383145 to 10.13881	-	-	0.2832731	-0.7436073 to 32.16494	-	-
1.5	Uniformity	Skewed	0.0075111	0.0042688 to 0.0261619	-	-	0.0068358	0.0041506 to 0.0223403	-	-
1.8	Entropy	Skewed	6.970371	5.103056 to 7.980835	-	-	7.196926	5.118563 to 7.999186	-	-
1.8	Uniformity	skewed	0.0095682	0.0047676 to 0.03125	-	-	0.0081453	0.0045229 to 0.032	-	-
2.0	Entropy	skewed	6.754185	4.47641 to 7.945526	-	-	7.092453	4.306257 to 7.910995	-	-
2.0	Uniformity	skewed	0.0112073	0.0052598 to 0.0519031	-	-	0.0089089	0.0048764 to 0.0535077	-	-
2.0	Mean Positive Pixels	skewed	20.71824	3.979074 to 64.27147	-	-	24.35689	7.737309 to 72.85161	-	-
2.5	Entropy	skewed	6.246424	2.75 to 7.831608	-	-	6.701752	3.970176 to 7.766553	-	-
2.5	Mean Positive Pixels	skewed	16.12741	3.635599 to 53.67281	-	-	20.03748	3.109656 to 47.58016	-	-

Table 3

Mean texture parameters for the largest cross section of process in the adrenal gland. Mean/Median, Std. error/Range and 95 % CI interval split on benign and malignant groups.

Table 3 Mean texture parameters for single slice										
Filter	Texture Parameter	Distribution	Mean/Median dependent on distribution							
			Benign	Range	Std. Error	95 % CI	Malignant	Range	Std. Error	95 % CI
Unfiltered	Mean	Gaussian	42.86289	–	1.582369	39.73741 to 45.98837	50.59692	–	1.894869	46.8542 to 54.33965
Unfiltered	Proportion Positive Pixels	Skewed	88.76812	59.91561 to 100	–	–	93.36016	62.6556 to 99.58333	–	–
Unfiltered	Mean Positive Pixels	Gaussian	50.79	–	1.31253	48.1975 to 53.38249	56.49708	–	1.597037	53.34263 to 59.65153
0.5	Entropy	Skewed	7.530872	6.372217 to 8.334802	–	–	7.637875	6.656484 to 8.482571	–	–
0.5	Uniformity	Skewed	0.0062144	0.003717 to 0.0133636	–	–	0.0058376	0.0032937 to 0.0113292	–	–
1.0	Entropy	Skewed	7.014068	4.932138 to 8.116034	–	–	7.349646	6.043462 to 8.102757	–	–
1.5	Entropy	Skewed	6.337024	3.906891 to 7.983215	–	–	6.942386	4.280395 to 7.771218	–	–
1.8	Entropy	Skewed	5.899018	3.169925 to 7.91784	–	–	6.710603	3.378783 to 7.679915	–	–
1.8	Uniformity	Skewed	0.0188118	0.005022 to 0.1111111	–	–	0.0116771	0.0059534 to 0.1020408	–	–
2.0	Entropy	Skewed	5.635905	2.321928 to 7.819547	–	–	6.491425	3.169925 to 7.658353	–	–
2.0	Uniformity	Skewed	0.0232097	0.0054211 to 0.2	–	–	0.0129062	0.0059375 to 0.1111111	–	–
2.5	Entropy	Skewed	4.865635	0 to 7.725908	–	–	5.908277	0 to 7.47352	–	–
2.5	Uniformity	Skewed	0.0382653	0.0056262 to 1	–	–	0.018843	0.0066207 to 1	–	–

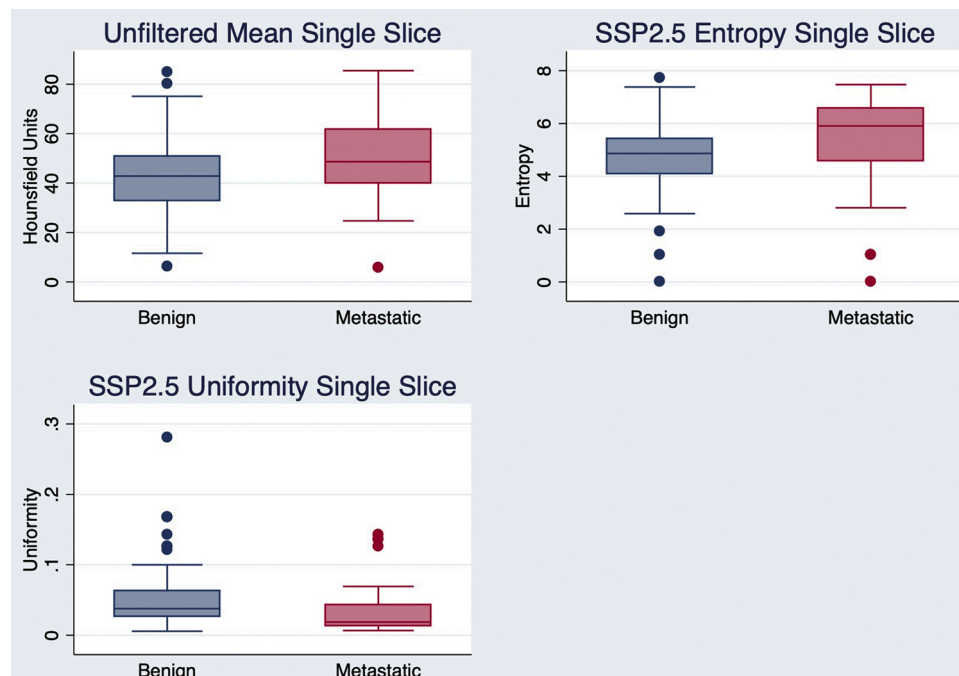


Fig. 3. Box-and-whisker plots split on benign and metastatic lesions for unfiltered mean single slice Hounsfield Units (Top left), course entropy single slice (Top right) and course uniformity single slice (Bottom left). All show considerable overlap between the groups despite them being statistically significant different.

3.6. Binary logistic regression

A binomial logistic regression showed the ability of the individual texture parameters to differentiate between malignant and benign adrenal glands. Initially all parameters were run individually as a univariate analysis, and showed area under the curve for receiver operating curves ranging from 36 % (Volume measurement kurtosis with a filter size of 0.5) to 69 % (Single slice entropy with a filter size of 2.5)

(Table 4).

3.7. Optimal model

As expected, several parameters showed good to excellent correlation; therefore, they cannot be combined for an optimal multivariate model. Based on the results from the binary logistic regression and correlation results the following texture parameters were selected for

Table 4
Results of the univariate binary logistic regression analysis including AUC results.

Filter	Texture parameter	Volume/single slice	Prob > chi2	Coefficient	Std. Error	p value	95 % conf interval	Area under ROC curve	Correctly classified
Unfiltered	Mean	single slice	0.0018	0.0333297	0.0111654	0.003	0.0114458 to 0.055235	0.6374	62.03%
Unfiltered	Proportion Positive Pixels	single slice	0.0030	0.0626225	0.0224558	0.005	0.01861 to 0.1066351	0.6438	64.68 %
Unfiltered	Mean Positive Pixels	single slice	0.0057	0.0350894	0.0131372	0.008	0.009341 to 0.0608379	0.6251	61.39%
0.5	Entropy	single slice	0.0145	0.9206986	0.3872393	0.017	0.1617235 to 1.679674	0.6014	56.96%
0.5	Uniformity	single slice	0.0222	-187.4358	85.07226	0.028	-354.1744 to -20.69723	0.5979	56.96%
1.0	Entropy	single slice	0.0009	1.01047	0.3244108	0.002	0.3746369 to 1.646304	0.6437	63.29%
1.5	Entropy	single slice	0.0011	0.6678778	0.2163842	0.002	0.2437726 to 1.091983	0.6641	67.09%
1.8	Entropy	single slice	0.0018	0.5282684	0.177987	0.003	0.1794204 to 0.8771165	0.6641	68.35%
1.8	Uniformity	single slice	0.0294	-21.40266	10.66993	0.045	-42.31534 to -0.4899691	0.6638	66.46%
2.0	Entropy	single slice	0.0009	0.5031505	0.1601617	0.002	0.1892393 to 0.8170618	0.6742	67.72%
2.0	Uniformity	single slice	0.0239	-15.42122	7.575771	0.042	-30.26946 to -0.5729847	0.6723	68.35%
2.5	Entropy	single slice	0.0023	0.3587023	0.1248687	0.004	0.1139642 to 0.6034404	0.6688	68.99%
2.5	Uniformity	single slice	0.6587	-0.5608435	1.293292	0.665	-3.09565 to 1.973963	0.6737	55.06%
Unfiltered	Mean	Volume	0.0003	0.0404208	0.0120166	0.001	0.0168687 to 0.0639729	0.6567	61.88%
Unfiltered	Mean Positive Pixels	Volume	0.0006	0.0464751	0.0143686	0.001	0.0183132 to 0.0746369	0.6493	60.62%
0.5	Kurtosis	Volume	0.3563	0.0572398	0.0572398	0.397	-0.0636668 to 0.1607 + 92	0.3560	53.12%
1.0	Kurtosis	Volume	0.4213	0.0379448	0.0499045	0.447	-0.0598662 to 0.1357557	0.3968	55.00%
1.5	Uniformity	Volume	0.0604	-103.3648	58.90883	0.079	-218.824 to 12.09437	0.5958	53.75%
1.8	Entropy	Volume	0.0178	0.6768651	0.296405	0.022	0.095922 to 1.257808	0.6196	58.13%
1.8	Uniformity	Volume	0.0422	-72.09075	37.62	0.055	-145.8246 to 1.643106	0.6232	58.13%
2.0	Entropy	Volume	0.0124	0.6239	0.2618195	0.017	0.1107433 to 1.137057	0.6401	61.25%
2.0	Uniformity	Volume	0.0630	-43.5771	25.56394	0.088	-93.68149 to 6.527296	0.6418	62.50%
2.0	Mean Positive Pixels	Volume	0.0104	0.0406122	0.0166854	0.015	0.0079093 to 0.0733151	0.6367	57.23%
2.5	Entropy	Volume	0.0196	0.4164133	0.1899238	0.028	0.0441694 to 0.7886572	0.6569	66.88%
2.5	Mean Positive Pixels	Volume	0.0572	0.0342292	0.0183925	0.063	-0.0018195 to 0.0702779	0.6191	57.96%

the multivariate analysis: single slice unfiltered mean, single slice entropy with a filter size of 2.5 and single slice uniformity with a filter size of 2.5. This showed that single slice unfiltered mean ($p = 0.009$), single slice entropy filter size 2.5 ($p < 0.005$) and single slice uniformity filter size 2.5 ($p = 0.013$) all significantly predict differentiation between malignant and benign adrenal gland lesions. The combined model has an area under the curve for the ROC at 73 % with a sensitivity of 58 %, specificity of 77 % and an overall accuracy of 68 %.

Based on the multivariate model a nomogram was generated to determine which lesions could be considered malignant by providing a percentage for risk of malignancy, however it did not add significant information (supplemental materials 3). Most likely due to the large overlap between the groups for the various parameters.

3.8. Supplemental materials

All texture features, pathology results and scanner types are supplied in supplemental materials as a CSV file.

4. Discussion

Using TexRAD software we found good to excellent stability of the texture parameters for both single slice and volume measurements. Several texture parameters showed significant difference between the two outcomes. After selection of parameters with high AUC values in binary logistic regression the optimal multivariate model using single slice unfiltered mean, single slice entropy filter size 2.5 and single slice uniformity filter size 2.5 show an AUC of 73 % and accurately classify 68 % of the cases.

A few studies have investigated the use of radiomics/texture analysis for characterization of adrenal gland lesions. In this study, we used scans from a series of different scanners on patients with adrenal lesions and primary lung cancer. All patients were scanned with the same protocol.

Prior studies have focused on several aspects of adrenal pathology. The primary publication from 2017 by Nakajo et al. focus on the ability of texture analysis to differentiate between F-18-fluorodeoxyglucose (FDG)-avid benign and metastatic adrenal tumors with PET/CT. They found that the combination of SUV_{max} and texture parameters significantly increase the diagnostic performance; however, the study includes relatively few patients (35 patients) and in our institution PET/CT is in

general not utilized before the contrast enhanced CT. Furthermore, the wait time for PET/CT is usually several days and the ability to determine if a biopsy should be performed or not prior to that is beneficial for the overall workup of the patients [20].

Tu *et al* found in 2018 that a combination of texture parameters and morphological imaging parameters could not reliably distinguish between malignant adrenal lesions and adenomas within a patient group diagnosed with primary lung cancer [16]. They found no significant difference between mean grey-level intensity (58.2 ± 21.0 HU for metastases vs 55.5 ± 21.5 HU, $p = 0.582$); however, Shi *et al.* in 2019 found metastases to have a significantly lower mean grey-level intensity and in the present study we find a significantly higher mean grey-level intensity in malignant adrenal lesions (50.60 CI95 % 46.85–54.34) compared to benign adrenal lesions (42.86 CI95 % 39.74–45.98). Furthermore, Shi *et al.* found significantly lower entropy and mean of positive pixels in the metastatic group compared to the benign lesions [15]. We found both entropy and mean to be higher in the metastatic group compared to the benign. Considering what is known regarding measurements on non-contrast scans and diagnosis of adrenal lipid rich adenomas as well as washout examinations for lipid poor adenomas we would expect lower mean grey-level intensity in the benign group as shown in our study [6,21].

We know from earlier studies that it is possible to use both the volume of a tumor or a single slice for texture analysis; however, in the adrenals it may be difficult to delineate the entire lesion without including normal adrenal tissue. In the present study we assessed two approaches: 1) encircling the entire adrenal gland (volume measurements) and 2) only the largest cross section area of the lesion within the adrenal (single slice measurements). Even though several parameters in both assessments show significant differences between metastatic and benign lesions in the adrenal, parameters for the largest cross section are more stable and produce higher AUC values compared to encircling the entire gland. Most likely this is caused by differences between normal adrenal gland tissue, which is included in the analysis, compared to tissue within the lesions. It is surprising that the differences are not greater than is shown here (Table 2 and 3).

The primary limitations of this study are the retrospective nature of the data and the lack of validation set from the study population. Our priority was to have a large sample size to provide the most optimal model for differentiation between metastatic and benign lesions in the adrenals. Furthermore, we included patients from regional areas and hospitals and several different scanner types and vendors. This presents as both a strength and a limitation as vendor specific reconstruction algorithms are used and scanner geometry most likely affect the texture parameters. However, it resembles our daily practice as close as possible.

In conclusion, we found several texture parameters statistically significantly different between metastatic and benign adrenal lesions in patients diagnosed with lung cancer. However, the most optimal AUC was only 73 %, so currently, the routine use of texture analysis to discriminate malignant from adrenal lesion cannot be recommended.

Source of funding

The authors have received salary from their individual institutions. No additional funding has been procured for the work presented in this manuscript.

CRedit authorship contribution statement

Michael Brun Andersen: Conceptualization, Methodology, Formal analysis, Data curation, Writing - original draft, Writing - review & editing, Visualization. **Uffe Bodtger:** Conceptualization, Data curation, Formal analysis, Writing - review & editing. **Iben Rahbek Andersen:** Data curation, Writing - review & editing. **Kennet Sønderstgaard Thorup:** Data curation, Formal analysis, Writing - review & editing.

Balaji Ganeshan: Software, Formal analysis, Data curation, Writing - review & editing. **Finn Rasmussen:** Conceptualization, Methodology, Writing - review & editing, Supervision.

Declaration of Competing Interest

One of the authors (BG) is the Co-founder /Co-inventor of TexRAD texture analysis software used in this study and a shareholder (not an employee) of Feedback Plc., a UK based company which owns, develops and markets the TexRAD texture analysis software.

All the other authors certify that they had complete control over the study and the results submitted.

The remaining authors declare that they have no competing interests

Appendix A. Supplementary data

Supplementary material related to this article can be found, in the online version, at doi:<https://doi.org/10.1016/j.ejrad.2021.109664>.

References

- [1] F. Bray, J. Ferlay, I. Soerjomataram, R.L. Siegel, L.A. Torre, A. Jemal, Global cancer statistics 2018: GLOBOCAN estimates of incidence and mortality worldwide for 36 cancers in 185 countries, *CA Cancer J. Clin.* 68 (6) (2018) 394–424.
- [2] Riis Rasmussen T., Jacobsen E., Rasmussen C., Madsen M. Årsrapport-2018_netudgave_rev.pdf [Internet]. https://www.lungecancer.dk/wp-content/uploads/2019/11/%C3%85rsrapport-2018_netudgave_rev.pdf. [henvist 6. oktober 2020]. Tilgængelig hos: https://www.lungecancer.dk/wp-content/uploads/2019/11/%C3%85rsrapport-2018_netudgave_rev.pdf.
- [3] Chatzellis E., Kaltsas G. Adrenal Incidentalomas. I: Feingold KR, Anawalt B, Boyce A, Chrousos G, de Herder WW, Dungan K, m.fl., redaktører. Endotext [Internet]. South Dartmouth (MA): MDText.com, Inc.; 2000 [henvist 11. september 2020]. Tilgængelig hos: <http://www.ncbi.nlm.nih.gov/books/NBK279021/>.
- [4] G.S. Chapman, D. Kumar, J. Redmond, S.H. Munderloh, D.R. Gandara, Upper abdominal computerized tomography scanning in staging non-small cell lung carcinoma, *Cancer* 54 (8) (1984) 1541–1543, 15. oktober.
- [5] S.E. Ettinghausen, M.E. Burt, Prospective evaluation of unilateral adrenal masses in patients with operable non-small-cell lung cancer, *J Clin Oncol Off J Am Soc Clin Oncol.* 9 (8) (1991) 1462–1466, august.
- [6] E.M. Caoili, M. Korobkin, I.R. Francis, R.H. Cohan, J.F. Platt, N.R. Dunnick, Adrenal masses: characterization with combined unenhanced and delayed enhanced CT, m.fl. *Radiology* 222 (3) (2002) 629–633, marts.
- [7] F. Fujiyoshi, M. Nakajo, Y. Fukukura, S. Tsuchimochi, Characterization of adrenal tumors by chemical shift fast low-angle shot MR imaging: comparison of four methods of quantitative evaluation, *Am J Roentgenol* 180 (6) (2003) 1649–1657, 1. juni.
- [8] G. Akkuş, İ.B. Güney, F. Ok, M. Evran, V. İzol, Ş. Erdoğan, Diagnostic efficacy of 18F-FDG PET/CT in patients with adrenal incidentaloma, m.fl. *Endocr. Connect.* 8 (7) (2019) 838–845, 28. maj.
- [9] P. Vilmann, P. Clementsen, S. Colella, M. Siemsen, P. De Leyn, J.-M. Dumonceau, Combined endobronchial and esophageal endoscopy for the diagnosis and staging of lung cancer: European Society of Gastrointestinal Endoscopy (ESGE) Guideline, in cooperation with the European Respiratory Society (ERS) and the European Society of Thoracic Surgeons (ESTS), m.fl. *Endoscopy* 47 (06) (2015) 545–559, 1. juni.
- [10] C.J. Tyng, A.G.V. Bitencourt, E.B.L. Martins, P.N.V. Pinto, R. Chojniak, Technical note: CT-guided paravertebral adrenal biopsy using hydrodissection—a safe and technically easy approach, *Br. J. Radiol.* 85 (1015) (2012) e339–42, juli.
- [11] K.A. Miles, B. Ganeshan, M.P. Hayball, CT texture analysis using the filtration-histogram method: what do the measurements mean? *Cancer Imaging* 13 (3) (2013) 400–406, 23. september.
- [12] F. Davnall, C.S.P. Yip, G. Ljungqvist, M. Selmi, F. Ng, B. Sanghera, Assessment of tumor heterogeneity: an emerging imaging tool for clinical practice?, m.fl. *Insights Imaging* 3 (6) (2012) 573–589, december.
- [13] R. Chowdhury, B. Ganeshan, S. Irshad, K. Lawler, M. Eisenblätter, H. Milewicz, The use of molecular imaging combined with genomic techniques to understand the heterogeneity in cancer metastasis, m.fl. *Br. J. Radiol.* 87 (1038) (2014), 20140065, juni.
- [14] L.M. Ho, E. Samei, M.A. Mazurowski, Y. Zheng, B.C. Allen, R.C. Nelson, Can Texture Analysis Be Used to Distinguish Benign From Malignant Adrenal Nodules on Unenhanced CT, Contrast-Enhanced CT, or In-Phase and Opposed-Phase MRI?, m.fl. *Am J Roentgenol.* 212 (3) (2019) 554–561, 8. januar.
- [15] B. Shi, G.-M.-Y. Zhang, M. Xu, Z.-Y. Jin, H. Sun, Distinguishing metastases from benign adrenal masses: what can CT texture analysis do? *Acta Radiol.* 60 (11) (2019) 1553–1561, 1. november.
- [16] W. Tu, R. Verma, S. Krishna, M.D.F. McInnes, T.A. Flood, N. Schieda, Can Adrenal Adenomas Be Differentiated From Adrenal Metastases at Single-Phase Contrast-Enhanced CT? *Am J Roentgenol.* 211 (5) (2018) 1044–1050, 12. september.
- [17] K. Sasaguri, N. Takahashi, M. Takeuchi, R.E. Carter, B.C. Leibovich, A. Kawashima, Differentiation of benign from metastatic adrenal masses in patients with renal cell

- carcinoma on contrast-enhanced CT, *Am J Roentgenol.* 207 (5) (2016) 1031–1038, 24. august.
- [18] I.S. Christiansen, K. Ahmad, U. Bødter, T.M.H. Naur, J.S. Sidhu, R. Nessar, EUS-B for suspected left adrenal metastasis in lung cancer, *m.fl. J. Thorac. Dis.* 12 (3) (2020) 258–263. marts
- [19] U. Bødter, P. Clementsen, J. Annema, P. Vilmann, Endoscopic ultrasound via the esophagus: a safe and sensitive way for staging mediastinal lymph nodes in lung cancer, *Thorac. Cancer* 1 (1) (2010) 4–8.
- [20] M. Nakajo, M. Jinguji, M. Nakajo, T. Shinaji, Y. Nakabeppu, Y. Fukukura, Texture analysis of FDG PET/CT for differentiating between FDG-avid benign and metastatic adrenal tumors: efficacy of combining SUV and texture parameters, *m.fl. Abdom. Radiol. N. Y.* 42 (12) (2017) 2882–2889.
- [21] M. Korobkin, F.J. Brodeur, I.R. Francis, L.E. Quint, N.R. Dunnick, F. Lundy, CT time-attenuation washout curves of adrenal adenomas and nonadenomas, *Am. J. Roentgenol.* 170 (3) (1998) 747–752, 1. marts.